Praseodymium polyhydrides synthesized at high temperatures and pressures

Miriam Peña-Alvarez,[1] Jack Binns,[2,*] Andreas Hermann,[1] Liam C. Kelsall,[1] Philip Dalladay-Simpson,[2] Eugene Gregoryanz,[1,2,†] and Ross T. Howie[2,‡]

[1]*Centre for Science at Extreme Conditions and School of Physics and Astronomy, University of Edinburgh, Edinburgh EH9 3FD, United Kingdom*

[2]*Center for High Pressure Science and Technology Advanced Research, Shanghai 201203, China*

(Received 4 June 2019; revised manuscript received 21 October 2019; published 13 November 2019)

Rare earth element polyhydrides have been predicted to exhibit high-T_c superconductivity at extreme compressions. Through a series of *in situ* high-pressure high-temperature x-ray powder diffraction experiments combined with density functional theory calculations, we report the emergence of polyhydride species in the praseodymium-hydrogen system. We initially observe the formation of PrH_3, which continuously increases in hydrogen content on compression towards PrH_4. Laser heating PrH_4 in a hydrogen medium at pressures of 85 GPa leads to the synthesis of both PrH_9 and PrH_7. Both structures are characterized by hexagonal arrays of praseodymium atoms surrounded by hydrogen clathrate cages.

DOI: 10.1103/PhysRevB.100.184109

I. INTRODUCTION

It has been postulated that the presence of heavy elements within a hydrogen lattice may provide chemical precompression, resulting in the dissociation of H_2 molecules at considerably lower pressure than expected for elemental H_2 [1]. These materials are generally referred to as hydrides or polyhydrides. They have captivated scientific experimental and theoretical attention in the last decade as they are predicted to show exotic properties such as metallicity and high-T_c superconductivity at conditions accessible with current experimental capabilities [2–5]. The most promising structural candidates are characterized by high-symmetry lattices of metal atoms surrounded by clathrate cages of hydrogen, allowing very high H content without forming H_2 molecules [6].

Rare-earth metals (REs) react with hydrogen to form cubic, nonstoichiometric hydrides [7–9]. When exposed to a hydrogen atmosphere and high-pressures, most of these hydrides can absorb additional hydrogen up to a composition limit of approximately REH_3 [10,11]. Through the combined application of pressure and temperature (above 100 GPa and 1000 K), new phases are expected to emerge with significantly higher hydrogen content. In particular, rare-earth hydrides (REHs) have emerged as the most promising candidates to form clathrate cages of H, which may present many attractive and novel properties [12,13]. For example, the combined high-pressure and high-temperature (laser heating) synthetic route has recently been used to form a superhydride, LaH_{10} [5]. It was later reported that this compound exhibits superconductivity at 260 K at pressures between 180–200 GPa [14,15].

Due to the identical structure of their outermost electron shells, rare-earth metals exhibit physical properties that depend only weakly on the occupancy of the $4f$ shell. Therefore, it should be expected that similar high-pressure and high-temperature routes would induce the formation of superhydrides in other rare-earth metals [11]. In particular, praseodymium polyhydrides have been predicted to show high-temperature superconductivity (T_c above 50 K) when the ratio H to Pr is above 9 [13]. Theoretical studies of the Pr-H system suggest that PrH_4 (space group $I4/mmm$) should be the most stable stoichiometry up to 50 GPa. Polyhydride species with H-rich cages are predicted to stabilize at higher pressure: PrH_8 ($P6_3mc$) at 100 GPa, PrH_9 ($F\bar{4}3m$) at 200 GPa, and only at around 400 GPa does the high-T_c PrH_{10} phase become energetically favoured [13]. A recent study reported the synthesis of PrH_9 at 115 GPa and 1650 K[16]. Two polymorphs, hexagonal $P6_3/mmc$ and cubic $F\bar{4}3m$, were produced in the pressure range between 115 and 125 GPa, however, the pressure stability ranges of such compounds were not fully explored.

Here, through a combination of high-pressure high-temperature experiments using x-ray diffraction as a diagnostic, combined with density functional theory (DFT) calculations, we report the synthesis and pressure-dependent behavior of previously unobserved praseodymium polyhydrides. We document the expected reaction of Pr and H_2 forming PrH_3 adopting $Fm\bar{3}m$ structure below 5 GPa. On compression, the H content of the PrH_3 species increases, exhibiting a continuous phase transition towards PrH_4 by 40 GPa. Laser heating this phase between 85–95 GPa leads to a radical transformation of the sample producing two new Pr-H compounds: PrH_9 and PrH_7. Both phases crystallize in hexagonal structures, distinguished by their different volumes and stabilities. PrH_9 contains PrH_{29} clusters and is stable from 76 GPa to at least 96 GPa. The secondary reaction product, PrH_7, contains PrH_{21} clusters and has a wider stability range from 96 GPa down to 60 GPa. The hexagonal structure of PrH_9 is unexpected, as former predictions suggested that a cubic structure should be observed instead [13]. These results demonstrate that the pressure-temperature-composition phase space of praseodymium hydrides is more complex than previously thought.

*Present address: School of Science, RMIT University, Melbourne, VIC 3000, Australia.

†e.gregoryanz@ed.ac.uk

‡ross.howie@hpstar.ac.cn

II. METHODS

High-purity Pr powder (99.5%, sim 40 mesh, Alfa-Aesar) was initially compressed into foils of approximately 8×8 μm and loaded into diamond anvil cells (DAC) together with a gold pressure marker [17]. The sample preparation was conducted in an inert environment glove box and the Pr foils were hermetically sealed within the Re gasket chamber. Research grade hydrogen (99.9999%) was subsequently gas loaded at a pressure of 0.17 GPa. Loading of hydrogen was confirmed by the observation of the hydrogen vibrational mode using a custom-built microfocused Raman system [18]. NH_3BH_3 has become a widely accepted method for *in situ* hydrogen generation to facilitate the synthesis of high-pressure polyhydrides [14–16,19]. However, using pure H_2 instead of NH_3BH_3 guarantees a higher density of hydrogen available to synthesize high-stoichiometry hydrides. Rhenium gaskets, indented to 9–18 μm thickness, were used to form the sample chamber in all experimental runs. The diamond anvil culets ranged from 50–100 μm, with sample sizes ranging between 20–60 μm once hydrogen was in the solid state. Once loaded, pressure was increased to above the hydrogen solidification point, and the Pr foil was hydrogenated over a period of 7–14 days before x-ray diffraction measurements were conducted. Angle-dispersive x-ray diffraction patterns were recorded on a MAR-555 detector with synchrotron radiation ($\lambda = 0.4115$ Å, 30 keV) at the ID15B beam line (ESRF, France). Two-dimensional image-plate data were integrated with DIOPTAS to yield intensity vs 2θ plots [20]. Diffraction patterns were indexed with CONOGRAPH, Le Bail refinement was carried out in JANA2006 [21–23].

Total energy calculations were carried out within the framework of DFT in conjunction with the projector-augmented wave (PAW) method and a plane wave basis, as implemented in the VASP code [24,25]. We used the PerdewBurke-Ernzerhof (PBE) exchange-correlation functional [26] and hard PAW data sets (cutoff radii: $r_{Pr} = 2.8\,a_B$, $r_H = 0.8\,a_B$) that included the Pr $5s^2 5p^6 6s^2 4f^3$ electrons in the valence space. Pure hydrogen phases I and III were modeled in an eight-molecule cell of $P6_3/m$ symmetry and a $C2/c$ phase, respectively. The plane wave cutoff energy was 800 eV and Brillouin zone sampling was done on regular k-point grids with separations of 0.033 $Å^{-1}$. Zero-point energy (ZPE) contributions were initially included to test the stability of the cubic vs hexagonal PrH_9 structures, however, it was found to make no difference. As such, ZPE effects were not included for the calculated stability ranges of other phases. Spin-orbit coupling was included in the calculations, and found to have minor effects on relative stabilities and electronic properties.

III. RESULTS AND DISCUSSION

At pressures above 5 GPa, x-ray diffraction patterns show only the presence of the known hydride PrH_3 with a fcc ($Fm\bar{3}m$) structure [$a = 5.2719(3)$ Å at 11.2 GPa]. The synthesis of PrH_3 under pressure from its constituents, appears to produce poorly crystalline samples, characterized by broad diffraction peaks and a rapid drop off in diffracted intensity with 2θ (Fig. 1). This PrH_3 phase, remains stable up to at least 30 GPa. However, on further compression, the associated changes in volume per Pr atom with pressure suggest a continuous increase in hydrogen content. The PrH_3 (002) (200) and (202) reflections split indicating a transition to a body-centred tetragonal structure [$a = 3.4547(4)$, $c = 5.0130(10)$ Å at 44.1 GPa]. Comparison with the volume calculated from the equations of state of the elements [27,28] suggests a hydrogen-content approaching PrH_4 by 40 GPa (Fig. 2). Increasing pressure sees the volume per Pr atoms rising above that of Pr + 4H, indicating the formation of a solid solution approximating PrH_{4+x} (Fig. 2). The formation of PrH_{4+x} is in agreement with computational studies predicting PrH_4 ($I4/mmm$) as the most stable low-pressure Pr hydride [13]. This PrH_{4+x} phase is also poorly crystalline, again characterized by broad diffraction peaks. Above 75 GPa we observe the emergence of additional broad weak peaks, which we tentatively index to a body-centered tetragonal cell [$a = 2.9926(7)$ $c = 5.6998(32)$ Å at 90.4 GPa] with a volume similar to that of PrH_{4+x} at the same pressure (25.330 and 25.523 $Å^3$, respectively) suggesting a sluggish transition to a new polymorph.

Laser heating of metals in a high-pressure hydrogen environment has been a successful synthetic tool to overcome kinetic barriers and promote the formation of metal hydrides with unexpected stoichiometries [4,5,30–34]. In this work, PrH_{4+x} in a H_2 medium was laser heated using a 1064 nm Nd:YAG laser at pressures above 85 GPa. Temperatures were held between 1000–1400 K for a period of 10 s. Diffraction patterns indicated no changes during heating beyond the thermal lattice expansion of PrH_{4+x}. However, on quenching, the sample showed radical transformations in the obtained diffraction patterns with no shift in pressure. As seen in Fig. 1 upon quenching, the low-intensity broad diffraction peaks of PrH_{4+x} were replaced by well-defined rings. Comparison of the ring textures indicated the presence of two new phases, and all the observed peaks could be indexed with two hexagonal unit cells: $a = 3.7022(1)$, $c = 5.5215(3)$ Å and a minor phase with unit cell: $a = 3.8535(4)$, $c = 4.6442(7)$ Å at 91.4 GPa (Fig. 1).

Examination of the unit-cell volumes with pressure provides the best available probe to estimate the stoichiometry of these compounds. The unit-cell volume of the major phase is clearly greater than that of the predicted stable phase at this pressure, PrH_8 [Fig. 2(a)], suggesting instead a stoichiometry of PrH_9. We have performed our own DFT geometry optimization calculations for our determined PrH_9 structure and find excellent agreement between the experimentally observed volumes and those theoretically derived [see Fig. 2(a)]. Interestingly, previous predictions report that PrH_9 should only adopt a cubic crystal structure ($F\bar{4}3m$) [13]. Instead, in agreement with Ref. [16], we find that PrH_9 also adopts a $P6_3/mmc$ structure, found experimentally in NdH_9 [35], ThH_9 [36], and for CeH_9 [19,37]. However, Ref. [16] find coexistence between both $P6_3/mmc$ and $F\bar{4}3m$ hydride phases through high-temperature synthesis at the higher pressure of 105 GPa, while we only observe the former structure at 85 GPa. As such, the $F\bar{4}3m$ PrH_9 must emerge only at pressures greater than 85 GPa.

The minor PrH_7 phase also displays a hexagonal structure, in agreement with a number of predicted stoichiometries in the range REH_{6-9} [13,38]. On the basis of our DFT geometry optimization and stability searches within the pressure range 50–100 GPa we find the closest agreement in volume with

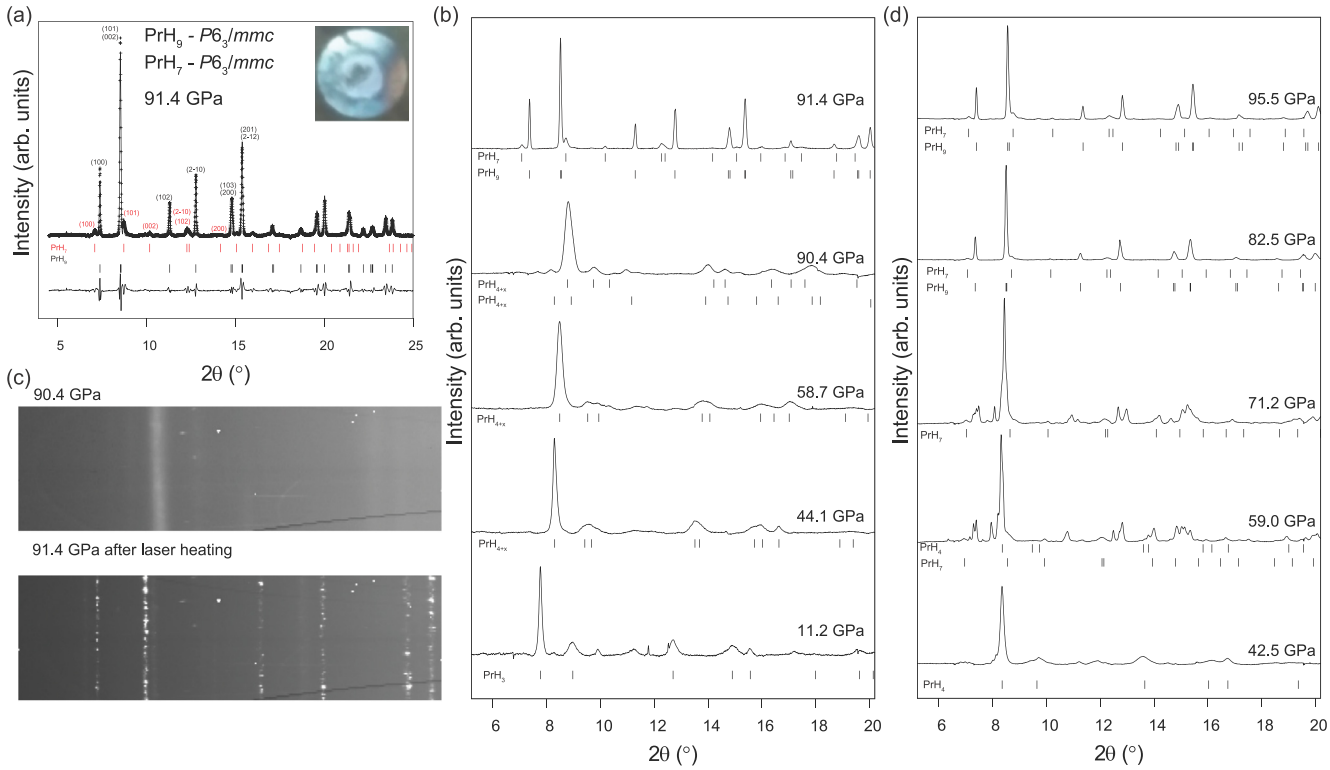

FIG. 1. (a) Representative Le Bail refinement of high-pressure x-ray diffraction data of PrH_7/PrH_9 mixture at 91.4 GPa. Tick marks indicate the calculated peak positions, the difference between observed and calculated profiles is shown below, $wR_p = 0.82\%$. Inset shows an image of the sample chamber at 20 GPa. Culet size is 50 μm; (b) High-pressure x-ray diffraction patterns ($\lambda = 0.4115$ Å) taken on compression showing the continuous transition from cubic ($Fm\bar{3}m$) PrH_3 to tetragonal ($I4/mmm$) PrH_4. Subsequent laser heating above 90 GPa leads to the synthesis of new praseodymium hydrides PrH_9 ($P6_3/mmc$) and PrH_7 ($P6_3/mmc$) as a minor phase; (c) X-ray diffraction patterns before and after laser heating; (d) Diffraction patterns taken on decompression showing the transition of PrH_9 from a hexagonal to a complex unknown structure below 82.5 GPa followed by its decomposition to PrH_4 below 59 GPa. PrH_7 remains stable down to 54 GPa. Both polyhydrides eventually decompose to PrH_4 with further decompression.

PrH_7 (see Figs. 2 and 3), isostructural to UH_7 [38]. The degree of mismatch between the predicted and experimentally observed PrH_7 volumes may suggest PrH_7 is a nonstoichiometric solid solution. However, confirmation of this would require neutron diffraction to determine hydrogen atomic positions, which is currently outwith experimental capabilities due to the pressures required for synthesis.

Figure 3(a) shows the full convex hulls of the Pr-H binary system at representative pressures. The relative formation enthalpies ΔH_f are with respect to decomposition into PrH and H_2, in the appropriate ratios. At 50 GPa, we find PrH_3, PrH_4, and PrH_8 stable, while PrH_7 (in the UH_7 structure type) is very close to stability. The latter, as well as PrH_3, becomes unstable at higher pressures. PrH_4 persists throughout the entire pressure range, while PrH_8 is predicted to be replaced by PrH_9 ($P6_3/mmc$ structure). It is interesting that high-temperature synthesis leads to the coexistence of both PrH_7 and PrH_9. In our calculations, both these phases are metastable at 85 GPa with respect to PrH_8 (Fig. 3), but they are not far off the stability region. Results at scalar-relativistic level (not shown) are very similar and agree very well with previous calculations [13], with the biggest difference being that PrH_7 is found to be stable up to 65 GPa. The hexagonal phase of PrH_9 is 0.35–0.45 eV/f.u. higher in enthalpy than the cubic phase in the pressure range 50–200 GPa; this is independent of whether spin-orbit coupling is considered or not.

Structure solution suggested Pr atoms to lie on special positions (2/3, 1/3, 1/4), resulting in *hcp* lattices. Data were not of sufficient quality for full Rietveld refinement and therefore utilized DFT geometry optimization calculations to confirm the formulas and structure of these phases (Table I). Both the PrH_7 and PrH_9 $P6_3/mmc$ structures consist of hexagonal

TABLE I. Crystal structure parameters for praseodymium polyhydrides optimized by DFT calculations including spin-orbit coupling at 80 GPa.

PrH_7 at 80 GPa	$a = 3.6070$ Å	$c = 5.4688$ Å	($P6_3/mmc$)
Atom	x	y	z
Pr1 (2d)	1/3	2/3	3/4
H1 (2b)	0	0	1/4
H2 (12k)	0.17499	0.34997	0.07268
PrH_9 at 80 GPa	$a = 3.5652$ Å	$c = 6.0943$ Å	($P6_3/mmc$)
Pr1 (2d)	1/3	2/3	3/4
H1 (2c)	1/3	2/3	1/4
H2 (4e)	0	0	0.16591
H3 (12k)	0.17694	0.35389	0.05950

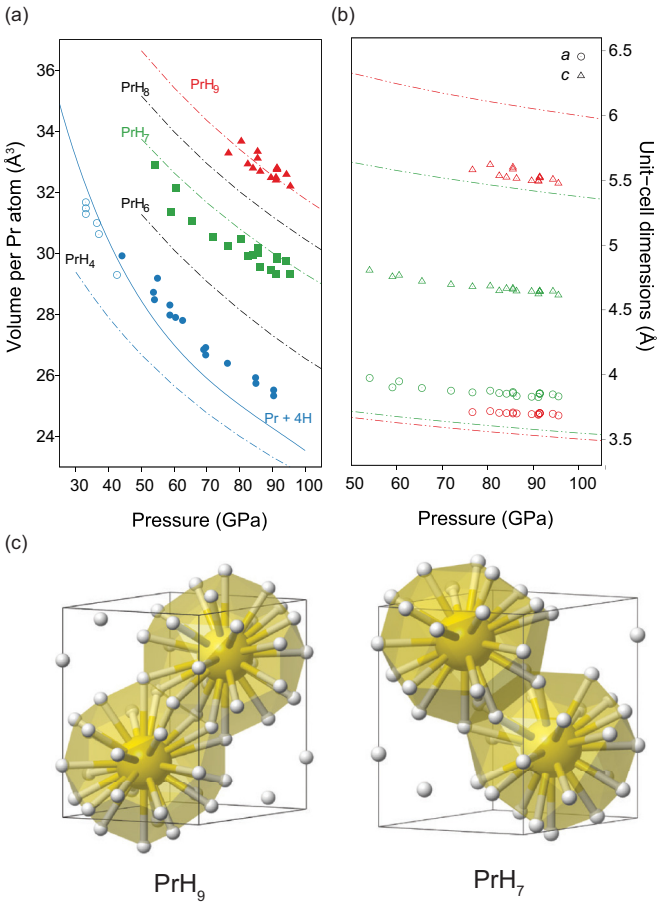

FIG. 2. (a) Volume per Pr atom for praseodymium hydrides. Empty circles correspond to the cubic phase of PrH_3. Filled blue circles correspond to high-pressure tetragonal PrH_{4+x} polymorph ($I4/mmm$). Solid line indicates volume derived from the atomic volumes of the elements [27–29], while dashed lines refer to volumes derived from our DFT calculations. (b) Unit cell parameters for PrH_7 (green) and PrH_9 (red). Dashed lines correspond to the DFT predicted values. (c) Crystal structures of Pr polyhydrides, PrH_7 ($P6_3/mmc$) and PrH_9 ($P6_3/mmc$); Pr atoms are yellow, H are white.

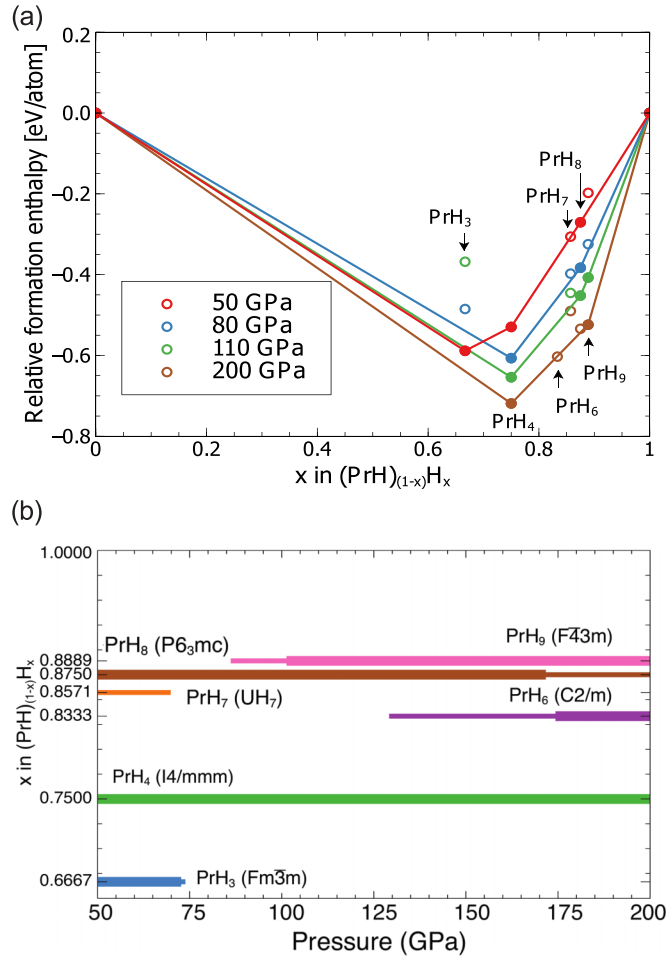

FIG. 3. (a) Convex hull construction for PrH_n phases relative to PrH and 1/2 H_2, at a sequence of pressures. Empty (filled) symbols denote metastable (stable) phases, the latter form the convex hull at each pressure. The stoichiometries considered are indicated. (b) Stability ranges of Pr-hydrides from spin-orbit coupling DFT calculations. Compositions and space groups/prototypes are indicated. Thin lines denote pressure ranges where the phases are metastable, defined as up to 10 meV/atom above the convex hull.

close-packed lattices of face-sharing Pr-H clusters. As seen in Fig. 2(b), in PrH_9 each Pr atom is surrounded by 29 H atoms, in PrH_7 the clusters consist of 21 H atoms. The electronic density of states (DOS) of these compounds are shown in Fig. 4, and compared both to PrH_4 and the cubic phase PrH_9-$F\bar{4}3m$. As seen, all the hydrides are very good metals. Hydrogen-richer hydrides have wider valence bands but the DOS at the Fermi level, which is dominated by Pr-f states, are not affected in a systematic way. Common structural features (atomic hydrogen clathrate cages encapsulating individual Pr atoms) and electronic properties (large DOS of similar character at the Fermi energy) suggest that electron-phonon coupling and therefore superconducting properties could be very similar across all of these superhydrides.

Samples of PrH_9 and PrH_7 were subsequently decompressed to establish the stability ranges of these new compounds. Diffraction peaks due to PrH_9 remain observable down to 80.5 GPa. Below this pressure peaks due to PrH_9 clearly split indicating a phase transition to yet another lower symmetry structure [Fig. 1(d)]. This low-symmetry phase is stable in a relatively narrow pressure range from 71.2–59 GPa. The diffraction peaks from this phase could not be indexed by any predicted RE-H structure, nor by any distorted subgroups of $P6_3/mmc$. Exhaustive searches with a number of indexing routines also failed to produce a convincing index, and the structure of this phase remains unknown. By contrast, PrH_7 retains its hexagonal symmetry until it too decomposes below 54 GPa, to the previously observed PrH_4 [Fig. 1(d)]. Former reports on PrH_x did not discuss the existence of PrH_7 [16] because as DFT calculations show, it is not favored above 75 GPa pressures, while experimentally we see it up to 95 GPa. However, these results demonstrate that measurements within the whole experimental pressure range are required for a full thermodynamic understanding of the reaction path. The use of NH_3BH_3 as hydrogen source is opening an avenue to many aspects of hydrogen-related high-pressure science as it avoids the

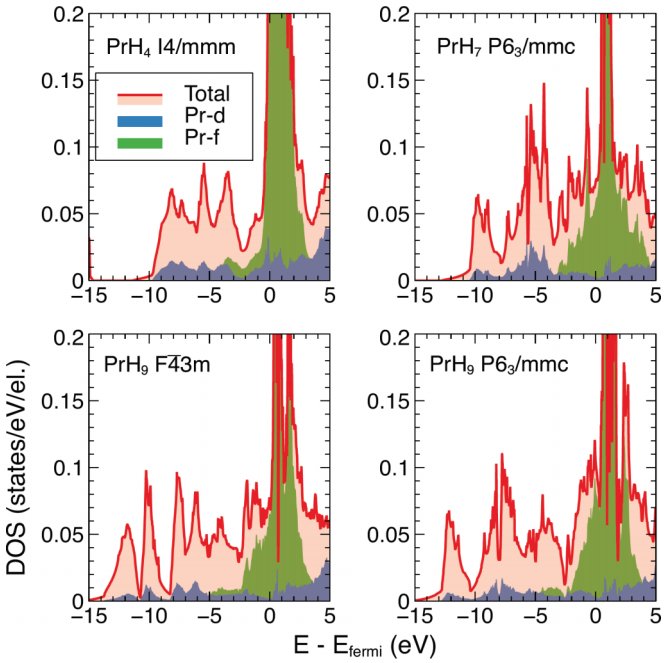

FIG. 4. Electronic densities of state (DOS) for PrH_4, PrH_7, PrH_9 ($F\bar{4}3m$), and PrH_9 ($P6_3/mmc$) from spin-orbit coupling calculations, all at 80 GPa.

requirement of H_2 gas loading. However, it is still a relatively new technique in the field, and it is not yet clear how side products such as BNH_x or BN [39] could interfere in the desired hydrogen-metal reaction or in the interpretation of the XRD patterns. Zhou *et al.* [16] and this present paper use NH_3BH_3 and H_2 gas loading, respectively. Both works find hexagonal PrH_9 at pressures around 100 GPa, therefore these results represent an important example where the same reaction product can be obtained using different hydrogen precursors.

IV. CONCLUSIONS

In conclusion, through laser heating a Pr foil within a pure H_2 atmosphere we have explored the Pr-H system up to pressures of 95 GPa with combined x-ray diffraction experiments and first-principles DFT calculations, unveiling the formation of polyhydride species. This work demonstrates that the formation of hydrogen-rich phases at extreme pressure-temperature conditions could potentially be realized in other REH compounds.

ACKNOWLEDGMENTS

The authors thank Prof. M. McMahon for access to facilities necessary for sample preparation. Authors acknowledge the European Synchrotron Radiation Facility for provision of synchrotron radiation facilities at the ID15B beam line under Proposal HC-3934. In particular, the authors acknowledge Dr. Michael Hanfland for his assistance during experiments. M.P.-A. would like to acknowledge the support of the European Research Council (ERC) Grant "Hecate" Reference No. 695527 secured by Graeme Ackland. Funding has been provided by the respective Chinese "1000 Talent Award" grants of both P.D.-S. and R.T.H. Computational resources provided by the UK's National Supercomputer Service through the UK Car-Parrinello consortium (EPSRC Grant No. EP/P022561/1) and by the UK Materials and Molecular Modelling Hub (No. EP/P020194) are gratefully acknowledged.

[1] N. W. Ashcroft, Phys. Rev. Lett. **92**, 187002 (2004).
[2] H. Wang, J. S. Tse, K. Tanaka, T. Iitaka, and Y. Ma, Proc. Natl. Acad. Sci. USA **109**, 6463 (2012).
[3] A. P. Drozdov, M. I. Eremets, I. A. Troyan, V. Ksenofontov, and S. I. Shylin, Nature (London) **525**, 73 (2015).
[4] C. Pépin, G. Geneste, A. Dewaele, M. Mezouar, and P. Loubeyre, Science **357**, 382 (2017).
[5] Z. M. Geballe, H. Liu, A. K. Mishra, M. Ahart, M. Somayazulu, Y. Meng, M. Baldini, and R. J. Hemley, Angew. Chem., Int. Ed. **57**, 688 (2018).
[6] H. Liu, I. I. Naumov, Z. M. Geballe, M. Somayazulu, J. S. Tse, and R. J. Hemley, Phys. Rev. B **98**, 100102(R) (2018).
[7] T. Palasyuk and M. Tkacz, Solid State Commun. **133**, 481 (2005).
[8] T. Palasyuk and M. Tkacz, Solid State Commun. **141**, 354 (2007).
[9] T. Palasyuk and M. Tkacz, Solid State Commun. **141**, 302 (2007).
[10] H. Müller, P. Knappe, and O. Greis, Z. Phys. Chem. **114**, 45 (1979).
[11] M. Mintz, Z. Hadari, and M. Bixon, J. Less-Common Met. **37**, 331 (1974).
[12] H. Liu, I. I. Naumov, R. Hoffmann, N. Ashcroft, and R. J. Hemley, Proc. Natl. Acad. Sci. USA **114**, 6990 (2017).
[13] F. Peng, Y. Sun, C. J. Pickard, R. J. Needs, Q. Wu, and Y. Ma, Phys. Rev. Lett. **119**, 107001 (2017).
[14] M. Somayazulu, M. Ahart, A. K. Mishra, Z. M. Geballe, M. Baldini, Y. Meng, V. V. Struzhkin, and R. J. Hemley, Phys. Rev. Lett. **122**, 027001 (2019).
[15] A. Drozdov, P. Kong, V. Minkov, S. Besedin, M. Kuzovnikov, S. Mozaffari, L. Balicas, F. Balakirev, D. Graf, V. Prakapenka *et al.*, Nature (London) **569**, 528 (2019).
[16] D. Zhou, D. Semenok, D. Duan, H. Xie, X. Huang, W. Chen, X. Li, B. Liu, A. R. Oganov, and T. Cui, arXiv:1904.06643 (2019).
[17] Y. Fei, A. Ricolleau, M. Frank, K. Mibe, G. Shen, and V. Prakapenka, Proc. Nat. Acad. Sci. USA **104**, 9182 (2007).
[18] P. Dalladay-Simpson, R. T. Howie, and E. Gregoryanz, Nature (London) **529**, 63 (2016).
[19] X. Li, X. Huang, D. Duan, C. J. Pickard, D. Zhou, H. Xie, Q. Zhuang, Y. Huang, Q. Zhou, B. Liu *et al.*, Nature Commun. **10**, 3461 (2019).
[20] C. Prescher and V. B. Prakapenka, High Press. Res. **35**, 223 (2015).
[21] R. Oishi-Tomiyasu, J. Appl. Crystallogr. **47**, 593 (2014).
[22] A. Le Bail, H. Duroy, and J. Fourquet, Mater. Res. Bull. **23**, 447 (1988).
[23] V. Petříček, M. Dušek, and L. Palatinus, Z. Kristallogr. Cryst. Mater. **229**, 345 (2014).

[24] G. Kresse and J. Furthmüller, Phys. Rev. B **54**, 11169 (1996).
[25] G. Kresse and D. Joubert, Phys. Rev. B **59**, 1758 (1999).
[26] J. P. Perdew, K. Burke, and M. Ernzerhof, Phys. Rev. Lett. **77**, 3865 (1996).
[27] P. Loubeyre, R. LeToullec, D. Hausermann, M. Hanfland, R. Hemley, H. Mao, and L. Finger, Nature (London) **383**, 702 (1996).
[28] S. R. Evans, I. Loa, L. F. Lundegaard, and M. I. McMahon, Phys. Rev. B **80**, 134105 (2009).
[29] B. J. Baer, H. Cynn, V. Iota, C.-S. Yoo, and G. Shen, Phys. Rev. B **67**, 134115 (2003).
[30] E. Gregoryanz, C. Sanloup, M. Somayazulu, J. Badro, G. Fiquet, H.-K. Mao, and R. J. Hemley, Nature Mater. **3**, 294 (2004).
[31] A. Marizy, G. Geneste, P. Loubeyre, B. Guigue, and G. Garbarino, Phys. Rev. B **97**, 184103 (2018).
[32] M. Wang, J. Binns, M.-E. Donnelly, M. Peña-Alvarez, P. Dalladay-Simpson, and R. T. Howie, J. Chem. Phys. **148**, 144310 (2018).
[33] J. Binns, M.-E. Donnelly, M. Wang, A. Hermann, E. Gregoryanz, P. Dalladay-Simpson, and R. T. Howie, Phys. Rev. B **98**, 140101 (2018).
[34] J. Binns, P. Dalladay-Simpson, M. Wang, G. J. Ackland, E. Gregoryanz, and R. T. Howie, Phys. Rev. B **97**, 024111 (2018).
[35] D. Zhou, D. V. Semenok, H. Xie, A. I. Kartsev, A. G. Kvashnin, X. Huang, D. Duan, A. R. Oganov, and T. Cui, arXiv:1908.08304.
[36] D. V. Semenok, A. G. Kvashnin, A. G. Ivanova, V. Svitlyk, V. Yu. Fominski, A. V. Sadakov, O. A. Sobolevskiy, V. M. Pudalov, I. A. Troyan, and A. R. Oganov, Mater. Today (2019), doi:10.1016/j.mattod.2019.10.005.
[37] N. P. Salke, M. M. D. Esfahani, Y. Zhang, I. A. Kruglov, J. Zhou, Y. Wang, E. Greenberg, V. B. Prakapenka, J. Liu, A. R. Oganov *et al.*, Nature Commun. **10**, 4453 (2019).
[38] I. A. Kruglov, A. G. Kvashnin, A. F. Goncharov, A. R. Oganov, S. S. Lobanov, N. Holtgrewe, S. Jiang, V. B. Prakapenka, E. Greenberg, and A. V. Yanilkin, Sci. Adv. **4**, eaat9776 (2018).
[39] J. Nylén, T. Sato, E. Soignard, J. L. Yarger, E. Stoyanov, and U. Häussermann, J. Chem. Phys. **131**, 104506 (2009).